PAPER

NJC
www.rsc.org/njc

Complexes of $(EtO)_2P(O)CH_2P(O)(OEt)_2$ with lanthanide nitrates

Anthony M. J. Lees,[a] Roman A. Kresinski[b] and Andrew W. G. Platt*[a]

[a] *School of Sciences, Staffordshire University, College Road, Stoke-on-Trent, UK ST4 2DE*
[b] *School of Chemical and Pharmaceutical Sciences, Kingston University, Penrhyn Road, Kingston upon Thames, UK KT1 2EE*

Received (in Durham, UK) 4th June 2004, Accepted 16th September 2004
First published as an Advance Article on the web 3rd November 2004

The preparation of complexes of $(EtO)_2P(O)CH_2P(O)(OEt)_2$ = L, with lanthanide nitrates is described. Stable complexes with composition $LnL_2(NO_3)_3$ can be isolated for Ln = La–Eu and fully characterised. For Ln = Gd–Lu solid compounds could not be isolated. Conductivity and ^{31}P NMR spectroscopy indicate structural changes in solution between the lighter and heavier lanthanides and, whilst electrospray mass spectrometry confirms a dramatic difference in behaviour with complexes of the heavier lanthanides readily decomposing *via* loss of $EtNO_3$, other experiments show that this does not occur under the conditions of complex formation. The single crystal X-ray structures for Ln = La and Sm show the nitrates and OEt groups to be in close proximity. The changes in spectroscopic properties correlate well with the difficulties in isolating the complexes of heavier metals, and are possibly due to the formation of dimeric complexes rather than loss of ethyl nitrate.

DOI: 10.1039/b408536a

1 Introduction

Complexes of lanthanide nitrates continue to attract attention as mimics for less accessible actinide complexes[1] of potential interest in nuclear waste treatment, and for their inherent interest in exploring structural variations amongst the 4f metals. Many multifunctional PO based ligands have been examined and the structures of their lanthanide[2–4] and actinide[5,6] complexes reported. Solvent extraction properties of a variety of organophosphorus compounds with f-block metals have also been examined.[7–13] Ligands in which a central methylene group is bonded to two electron withdrawing phosphoryl groups have been previously explored as extractants. Solvent extraction studies of lanthanides with tetra(*p*-tolyl)methylene diphosphine dioxide,[10] where no complexes were isolated, indicate that compounds with 4 : 1 ligand to metal ratios for lighter lanthanides and 3 : 1 ratios for heavier lanthanides are formed. In further studies diphosphine dioxides, $R_2P(O)CH_2P(O)R_2$ and related ligands were examined in solution by EXAFS.[14] With R = *p*-tolyl holmium nitrate forms 2 : 1 complexes, whilst for R = octyl 1 : 1 complexes were formed. Powder X-ray diffraction studies of complexes of lanthanide nitrates with $(RO)_2P(O)CH_2P(O)(OR)_2$ (R = ^{i}Pr) indicated that complexes are formed in three structural classes La → Nd, Sm → Tb and Dy → Yb, although no single crystal data were reported.[15] The recent structural characterisation of 1 : 1 and 2 : 1 complexes of La and Pr nitrate complexes with $(^i PrO)_2P(O)CH_2P(O)(O^iPr)$[16] and the fact that complexes with $(^i PrO)_2P(O)(CH_2)_nP(O)(O^iPr)_2$ ligands with $n = 1$ were found to be much better extractants for lanthanide metals than with higher values of n,[17] prompted us to carry out a structural study on related complexes in order to characterise the transition points between the structures formed along the lanthanide series. Our past studies with bis-phosphonate lanthanide complexes have indicated a marked decrease in their stability for the heavier lanthanides,[18] and it is thus of interest from the point of view of reusability of the extractant to determine whether similar effects occur here. We chose to examine complexes of $(EtO)_2P(O)CH_2P(O)(OEt)_2$ = L, as this offers a less sterically congested outer coordination sphere, meaning any structural changes observed would be mainly due to the influence of primary coordination sphere effects. Additionally, smaller alkyl chains should lead to more crystalline products, perhaps allowing single crystal X-ray diffraction studies to be carried out.

2 Results and discussion

2.1 Synthesis

The reactions of lanthanide nitrates with L were carried out in trimethyl orthoformate solution as an *in situ* dehydration agent and afford a series of compounds of general formula $LnL_2(NO_3)_3$ for Ln = La – Eu. Much like the complexes of the hydroxydiphosphonate $[(MeO)_2P(O)]_2C(OH)R$ (= L′) from acetonitrile solution,[18] the yield is seen to decrease markedly with the increasing atomic mass of the lanthanide. Characterising data are given in Table 1. Analytically pure samples of the complexes of the lighter lanthanides (La–Sm) crystallized spontaneously from a solution of the reagents. The heavier lanthanides (Eu–Lu) behaved differently. They did not crystallise spontaneously from trimethyl orthoformate solution, but on addition of diethyl ether, oils having the characteristic colour of the lanthanide ion were precipitated. A solid material was obtained on trituration of the europium containing oil with diethyl ether, and the gadolinium complex reached a waxy semi-solid consistency with similar treatment, but satisfactory elemental analyses could be obtained for the La–Eu complexes only. The oils obtained for the heavier lanthanides could be crystallised neither from any common organic solvents, nor on prolonged drying. The infrared spectrum of the Yb containing oil is very similar to those obtained from the crystalline complexes discussed below. The trend in the melting points of the crystalline solids is linear with an approximately 5 °C decrease per lanthanide, with the formation of much lower melting point materials after Eu/Gd implying a significant structural change.

2.2 Solid state structures

2.2.1 Infrared spectroscopy. The infrared spectra of all of the solid complexes (as KBr discs) show a shift in the P═O stretching frequency from 1257 cm^{-1} in the free ligand, to

Table 1 Characterising data for $LnL_2(NO_3)_3$

		Elemental Analysis: Found (calc)/%				^{31}P NMR[a]	
Ln	Typical Yield/%	C	H	N	Mp/°C	δ/ppm	$\Delta\nu_{1/2}$/Hz[b]
La	93	23.91(23.99)	4.96(4.92)	4.60(4.66)	120.5	21.3	< 5
Ce	84	23.90(23.95)	4.92(4.91)	4.62(4.66)	114.2	42.0	10
Pr	76	23.92(23.93)	4.92(4.91)	4.55(4.65)	109.7	68.7	25
Nd	72	23.84(23.84)	4.89(4.89)	4.55(4.63)	103.4	77.7	35
Sm	62	23.61(23.68)	4.86(4.86)	4.59(4.60)	90.6	21.4	< 5
Eu	48	23.45(23.64)	4.82(4.85)	4.58(4.60)		−71.3	195

[a] Proton decoupled spectra. 50 mg/3 g $CDCl_3$. All solutions showed a single peak. [b] Linewidth at half height.

$\sim$1210 cm^{-1} in the complexes, indicating coordination *via* both phosphoryl oxygen atoms. The observed decrease in frequency is similar to that reported for the tetraisopropyl analogues.[15] The spectra all show the nitrate $\nu_1(A_1)$ and $\nu_5(B_2)$ bands at $\sim$1305 cm^{-1} and $\sim$1465 cm^{-1} consistent with nitrates being bound in a bidentate chelating manner. The splitting of the nitrate bands, $\Delta\nu$, shows a steady decrease form La to Eu. The ν_4 band of the nitrate ion also splits on adoption of C_{2v} symmetry: the combination band $\nu_1 + \nu_4$ at 1700–1800 cm^{-1} reflects this splitting and the separation of these two bands has previously been used to establish the mode of nitrate coordination.[19] The splitting of these bands in the spectra of the solid complexes obtained (29–44 cm^{-1}) is again consistent with bidentate coordination. In all of the spectra the band at $\sim$1465 cm^{-1} appears as a sharp doublet. Similar effects have been observed previously and have been attributed to non-equivalence of nitrate groups within either the crystal or the molecule.[15]

Infrared spectra obtained on the crystalline complexes under higher resolution ($\pm$2 cm^{-1}) and with no sample pretreatment resolve the PO absorption into 3 (La–Nd) and 2 (Sm) bands. This is consistent with the crystallography (discussed below) which shows 3 distinct PO distances for the La complex and 2 for the more symmetrical Sm complex. Interestingly the spectrum of the oil obtained from the $Yb(NO_3)_3$ reaction resembles that of the La complex in the PO region with 3 absorptions at similar frequencies and relative intensities. The NO absorptions are, however, significantly different from those of the La–Sm complexes and show two intense bands centred at 1491 and 1297 cm^{-1} suggesting a change in the nitrate environment. The magnitude of the splitting is larger than that observed for the La–Sm complexes (171–158 cm^{-1}) yet is still indicative of bidentate nitrate.

Infrared spectra of the Yb complex in $CDCl_3$ were examined and show a smaller splitting of the N–O peaks compared with the neat oil, at 168 compared with 194 cm^{-1}, whilst the PO region shows no significant difference. Interestingly there is no peak which could be assigned to a pendant PO group from a monodentate ligand or from an ionic nitrate.

Reaction of $Er(NO_3)_3$ with L in a 1 : 1 ratio produced an oil which solidified on standing. The product was partially soluble on addition of $CDCl_3$ and the transmittance infrared spectrum of the resulting suspension was similar to that of the Yb complex. On addition of L to the suspension a clear solution was formed whose infrared spectrum was identical to that of the original suspension. It seems that the heavier lanthanides also form 2 : 1 complexes and that the material isolated from the 1 : 1 reaction is a mixture of $Er(NO_3)_3$ and $ErL_2(NO_3)_3$ rather than a discrete 1 : 1 complex.[16]

2.2.2 Single crystal X-ray crystallography. Crystals of the lanthanum and samarium complexes were chosen for structural analysis, since they represent the complete span of the series for which crystalline materials could be obtained and, thus, their structures may indicate underlying reasons for the changes in properties along the lanthanide series. Although both complexes have similar overall molecular geometries, the samarium complex has a C_2 axis of symmetry passing through the N(1) nitrate ligand along the Sm···N(1)–O(4) line. One half of the N(1) nitrate, and the other two complete pairs of ligands are related by symmetry with equivalent atoms generated by the transformation $1 - x$, y, $3/2 - z$. This symmetry is not apparent in the lanthanum complex. The molecular structure of $LaL_2(NO_3)_3$ is shown in Fig. 1, details of the data collection and refinement are given in Table 2 and selected bond lengths and angles in Table 3.

The complexes adopt structures which are very similar to the tetraethylmalondiamide complex, $La\{[(Et_2N)C(O)]_2CH_2\}_2(NO_3)_3$[20] and to the recently published La and Pr tetraisopropylmethylene diphosphonates.[16] The La–O(P) distances are slightly smaller, ranging from 2.464(3)–2.515(3) Å for the lanthanum complex compared with a range of 2.511(2)–2.546(2) Å, these differences reflecting the reduced steric demands of the ethyl relative to the isopropyl groups. The metals are ten-coordinate with the nitrate and the diphosphonate ligands each chelating through two oxygen atoms. The coordination polyhedron around the metal in each complex can be considered to be a distorted bi-capped square antiprism as shown in Fig. 2. The distortion here can be attributed solely to the small bite of the nitrate ligands. The La and Sm complexes can also be considered as pseudo-pentagonal bipyramids, defined by the N-atoms of the nitrates and the phosphoryl oxygens. Two nitrates are axial and one equatorial with the PO oxygen atoms forming the other 4 positions in the equatorial plane. The inter-ligand repulsions, particularly between the positively charged N and P centres generally increase between La and Sm. With the exception of the shortest P···P distances which increase from 5.3990(17) Å (La) to 5.7002(29) Å (Sm), the repulsions between the N and P atoms increase from La

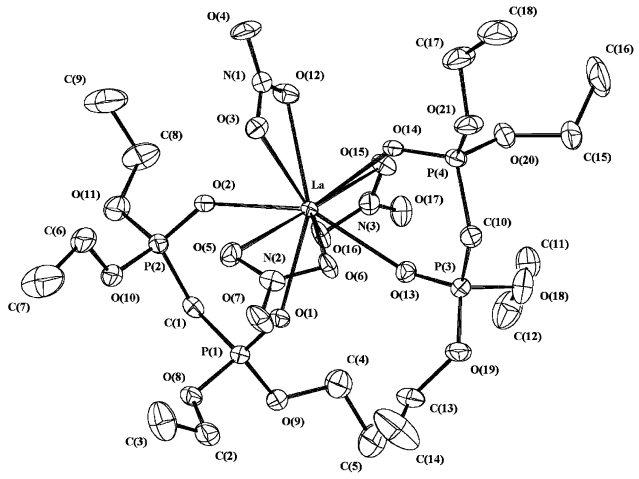

Fig. 1 The structure of $LaL_2(NO_3)_3$ with 50% probability ellipsoids, showing the atom-labelling scheme. H atoms have been omitted for clarity. Generated using SNOOPI.[38]

Table 2 Crystal data, data collection and refinement parameters

Compound	[La(CH_2{EtO_2PO}$_2$)$_2$(NO_3)$_3$]	[Sm(CH_2{EtO_2PO}$_2$)$_2$(NO_3)$_3$]
Empirical formula	$C_{18}H_{44}LaN_3O_{21}P_4$	$C_{18}H_{44}N_3O_{21}P_4Sm$
Molecular weight, M_r	901.35	912.79
Crystal system	monoclinic	monoclinic
Space group	$P2_1/c$	$C2/c$
Unit cell dimensions		
a (Å)	8.8205(11)	9.6295(2)
b (Å)	20.0885(6)	21.7274(4)
c (Å)	20.6300(14)	17.2755(3)
β (°)	91.716(16)	96.6898(10)
Cell volume, U (Å^3)	3653.8(5)	3589.8(12)
T (K)	293(2)	120(2)
Formula units/unit cell, Z	4	4
μ (mm^{-1})	1.425	1.896
Measured reflections	15032	18874
Independent reflections	5518	4117
R_{int}	0.0846	0.0530
Final R indices[a] ($F_o > 4\sigma(F_o)$)		
R (F)	0.0365	0.0448
wR_2 (F^2)	0.0833	0.1159
Final R indices[a] (all data)		
R (F)	0.0464	0.0429
wR_2 (F^2)	0.0853	0.1153

[a] $R = \Sigma||F_o| - |F_c||/\Sigma|F_o|$; $wR_2 = [\Sigma[w(F_o^2 - F_c^2)^2]/\Sigma[w(F_o^2)^2]]^{0.5}$.

to Sm, with P···N decreasing from 4.2635(36) Å (La) to 4.0378(47) Å (Sm) and N···N from 4.6918(54) Å (La) to 4.4872(70) Å (Sm). Similarly the P···Ln and N···Ln distances show significant changes, decreasing from 3.744(1) (La) to 3.707(2) (Sm) and 3.039(4) (La) to 2.987(6) (Sm), respectively.

The coordination of the nitrate groups is of interest: the N(1) nitrates in both the structures in the present study bond to the lanthanide such that the metal and the four atoms of the nitrate ion lie in essentially the same plane, the deviation being at most 0.050 Å for O(4) in the La structure, equating to a bending along the O(3)···O(12) line of 4.32(13)°. The bonding of the other nitrate groups in $LaL_2(NO_3)_3$ show greater deviation from their mean plane, due to a greater degree of bending along the line connecting their ligating O-atoms; this angle is 16.91(11)° for the N(2) group and 15.32(11)° for the N(3) group. Such deviations are not unprecedented; all of the similar L′ complexes[18] show some degree of nitrate group bending (10.96(20)° along O(3)···O(4) of the lanthanum complex) with an angle of 14.2° for the nitrate groups of Dy(phen)$_2$(acac)(NO$_3$)$_2$.[21] The nitrate groups of La[{$Et_2NC(O)$}$_2$$CHCH_2$-$CH_2OCH_2CH_3$]$_2$($NO_3$)$_3$[22] similarly display a marked inclination, the greatest bending in this case being 18.2°. In addition to the bending along the O···O line, the nitrate groups show varying degrees of asymmetry in their bidentate Ln–O(N) bonds. The N(1) nitrate group in the Sm complex is symmetrically coordinated, whereas all the other nitrate groups exhibit unequal Ln–O(N) bond lengths. Differences in the lengths of the two Ln–O(N) bonds are much greater in the Sm complex (about 0.2 Å in the bonding of the N(2) nitrate) compared with values ranging from 0.02 to 0.08 Å in the La complex. Asymmetry in the N–O(Ln) distances is likewise much less pronounced with only small differences (0.02 and 0.004 Å) being observed in the La complex.

There are weak intermolecular interactions between the oxygen atoms of the nitrates and methylene protons of the ethoxy groups. These interactions are stronger for the Sm complex with the O(3)···H(6A) and O(7)···H(8′2) distances being 2.386(4) Å and 2.388(5) Å compared with the closest contact in the La complex being between O(17)···H(6B) at 2.476(3) Å.

Table 3 Bond lengths, selected non-bonding distances and bond angles of $LnL_2(NO_3)_3$ (Å, °)

	La	Sm	
Ln–O(1)	2.501(3)	2.431(4)	
Ln–O(2)	2.464(3)	2.432(3)	
Ln–O(3)	2.566(3)	2.516(4)	
Ln–O(5)	2.683(3)	2.507(4)	
Ln–O(6)	2.602(3)	2.708(4)	
La–O(12)	2.601(3)	2.516(4)	Sm–O(3)^i
La–O(13)	2.502(3)	2.431(4)	Sm–O(1)^i
La–O(14)	2.515(3)	2.432(3)	Sm–O(2)^i
La–O(15)	2.638(3)	2.507(4)	Sm–O(5)^i
La–O(16)	2.617(3)	2.708(4)	Sm–O(6)^i
Ln···N(1)	3.016(4)	2.935(7)	
Ln···N(2)	3.060(4)	3.039(4)	
La···N(3)	3.042(4)	3.039(4)	Sm···N(2)^i
Ln···P(1)	3.762(1)	3.701(2)	
Ln···P(2)	3.717(1)	3.712(1)	
La···P(3)	3.752(1)	3.701(2)	Sm···P(1)^i
La···P(4)	3.748(1)	3.712(1)	Sm···P(2)^i
P(1)–O(1)	1.480(3)	1.478(4)	
P(1)–O(8)	1.553(3)	1.564(4)	
P(1)–O(9)	1.567(3)	1.565(4)	
P(1)–C(1)	1.796(4)	1.797(6)	
P(2)–O(2)	1.481(3)	1.475(4)	
P(2)–O(10)	1.551(3)	1.554(5)	
P(2)–O(11)	1.560(3)	1.538(6)	
P(2)–C(1)	1.788(4)	1.789(6)	
P(3)–O(13)	1.479(3)	1.478(4)	P(1)^i–O(1)^i
P(4)–O(14)	1.473(3)	1.475(4)	P(2)^i–O(2)^i
O(1)–Ln–O(2)	74.87(9)	74.13(12)	
O(1)–Ln–O(3)	130.18(9)	145.57(12)	
O(1)–Ln–O(5)	67.38(9)	73.74(13)	
O(1)–Ln–O(6)	75.70(9)	112.86(13)	
O(2)–Ln–O(3)	76.99(9)	74.54(13)	
O(2)–Ln–O(5)	72.38(9)	70.55(13)	
O(2)–Ln–O(6)	120.11(9)	107.97(12)	
O(3)–Ln–O(5)	65.27(10)	82.69(15)	
O(3)–Ln–O(6)	84.25(10)	64.62(15)	
O(5)–Ln–O(6)	48.28(9)	48.50(12)	
O(1)–P(1)–C(1)	112.71(18)	113.3(3)	
O(2)–P(2)–C(1)	112.31(18)	112.7(2)	
P(1)–O(1)–Ln	140.41(16)	141.2(2)	
P(2)–O(2)–Ln	139.54(16)	142.4(2)	
P(1)–C(1)–P(2)	113.4(2)	112.7(3)	

Symmetry Code: (i) $1 - x$, y, $3/2 - z$.

Whilst the absolute strength of these contacts is doubtless not great, their existence coincides with the difficulties in isolating complexes for the elements following samarium and the tendency for similar complexes to decompose *via* loss of alkyl nitrate, and we conclude that the intermolecular hydrogen bonding between the coordinated nitrate and OCH_2 contributes to the ease of decomposition. On heating the solid Sm complex to 175 °C the solid firstly melts and then resolidifies producing ethyl nitrate during the course of these changes. This was detected by the gas phase infrared spectrum which showed absorptions at 3004(w), 1663(vs), 1652(vs), 1294(s), 1285(s), 1025(m), 912(m) and 853(s) in excellent agreement with the literature values.[23]

2.2.3 Solution structures. Most techniques for studying solution properties of lanthanide complexes give only indirect information. Here the lability and paramagnetism of many of

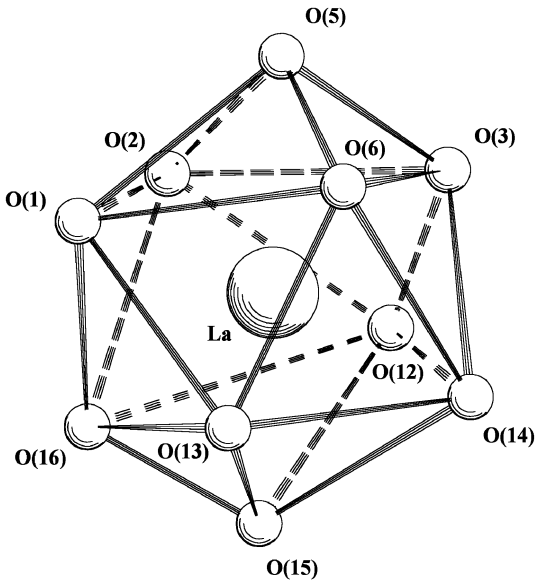

Fig. 2 Coordination geometry about the lanthanum atom of $LaL_2(NO_3)_3$.

the complexes make interpretations more difficult. We have used a combination of ^{31}P NMR spectroscopy, conductivity and electrospray mass spectrometry in an attempt to gain insight into the changes in solution structures which may accompany the transition from crystalline complexes of the lighter lanthanides to non-crystalline materials for their heavier counterparts.

2.2.3.1 ^{31}P NMR spectroscopy. The proton decoupled ^{31}P NMR spectra of the complexes all show single peaks. Since solid complexes were only isolated for the lanthanides La → Eu, ^{31}P NMR data were collected for the remainder of the series by dissolving stoichiometric amounts of nitrate and diphosphonate in deuterochloroform in the manner used previously for the analogous L′ complexes.[18]

Lanthanide induced shift analysis applied to this data indicates that there is a structural change in solution between the lighter lanthanides (La–Sm) and the heavier ones (Eu–Lu). Plots of $\delta_i/\langle S_z\rangle_i$ *versus* $D_i/\langle S_z\rangle_i$ and δ_i/D_i *versus* $\langle S_z\rangle_i/D_i$ (where the paramagnetic shift $\delta_i = \delta_{Ln} - 0.5(\delta_{La} + \delta_{Lu})$ and where δ_{Ln} is the observed shift for the Ln complex; $\langle S_z\rangle_i$ are the spin expectation values and D_i a parameter related to the variation in δ_i which should occur if the crystal field coefficients are independent of the lanthanide ion respectively[24]), have two linear regions with breaks between Sm and Eu, indicating a major change in solution structure. These are shown in Fig. 3. These results are from the analysis of one nucleus in the compounds, the analysis of two nuclei[25] has been shown to give more reliable results and the conclusions based on the current NMR analysis must be considered as tentative.

2.2.3.2 Conductivity. Although limited to the first half of the series, the trend in molar conductance (at a concentration of approximately 1 mM in acetonitrile) as the series is traversed follows the same pattern previously observed for the analogous L′ complexes:[18] a steady increase to samarium followed by a decrease at europium as shown in Fig. 4. The values of molar conductance, 12–25 Ω^{-1} cm^2 mol^{-1} are low compared to those expected for 1 : 1 electrolytes in acetonitrile (120–160 Ω^{-1} cm^2 mol^{-1} [26]) and suggest that there is little dissociation of the molecular species $LnL_2(NO_3)_3$. The increasing conductivity from La to Sm could be due to increasing steric crowding of the complexes being relieved by ionisation of nitrate in solution:

$$Ln(\kappa^2L)_2(NO_3)_3 \rightleftarrows [Ln(\kappa^2L)_2(NO_3)_2]^+ + [NO_3]^-.$$

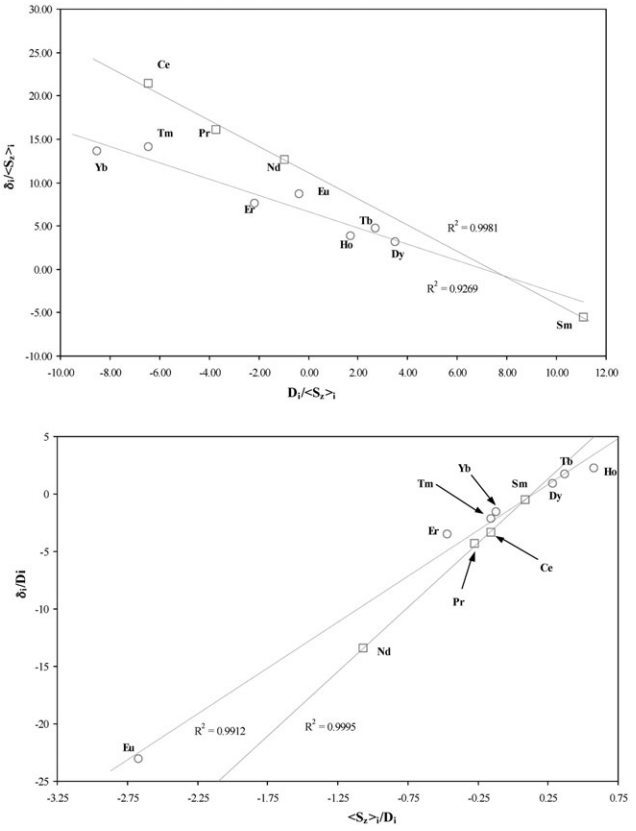

Fig. 3 Lanthanide Induced Shift plots for $LnL_2(NO_3)_3$ in $CDCl_3$ solution.

For Eu and possibly onwards, the decrease could be explained by a different mechanism for the reduction in steric crowding involving the phosphoryl groups bridging to form a less congested dimer, competing with the above and reducing the overall conductivity:

$$2\ Ln(\kappa^2L)_2(NO_3)_3 \rightleftarrows Ln(\kappa^2L)(NO_3)_3(\mu L)_2Ln(\kappa^2L)(NO_3)_3.$$

Precedent for this type of bridging has recently been reported in UO_2^{2+} complexes with $[Ph_2P(O)]_2CH_2$.[27]

The alternative means of reducing in the crowding of the first coordination sphere achieved by dissociation of L, is felt to be less likely as the infrared spectra of $Yb(NO_3)_3L_2$ either as the neat oil or in $CDCl_3$ solution, give no indication of the presence of a pendant phosphoryl group or free nitrate ion, the absorption profile in the PO region being very similar to that observed for the La complex. The possibility of forming nitrate bridged dimers, $Ln(\kappa^2L)_2(NO_3)_2(\mu NO_3)_2Ln(\kappa^2L)_2(NO_3)_2$ analogous to the solid state structures of the 1 : 1 complexes of $La(NO_3)_3$ and $Pr(NO_3)_3$ with (^{i}PrO)$_2$P(O)CH^{2}P(O)(O^{i}Pr)$_2$[16] seems less likely to be the reason here,

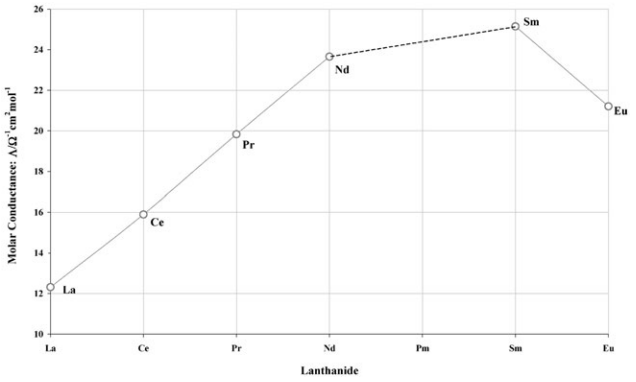

Fig. 4 Molar conductance of $LnL_2(NO_3)_3$ in acetonitrile @ 0.001 M.

Table 4 Positive ion electrospray mass spectral data[a] (+20 V) for $LnL_2(NO_3)_3$ in methanol

	La	Pr	Nd	Sm	Yb
$[LnL_3]^{3+}$	334.5(30)	335.1(35)	336.1(30)		346.0(5)
$[LnL_4]^{3+}$	430.6(65)	431.2(55)	432.2(50)	434.9(5)	442.1(15)
$[Ln(NO_3)L_2]^{2+}$	388.7(15)	389.5(10)			
$[Ln(NO_3)L_3]^{2+}$	532.7(100)	533.7(100)	535.2(100)	539.1(30)	550.2(35)
$[Ln(NO_3)L_3–EtNO_3]^{2+}$				493.7(100)	504.7(100)
$[Ln(NO_3)_2L_2]^{+}$	839.2(20)	841.2(25)	844.3(30)	852.2(20)	
$[Ln(NO_3)_2L_2–EtNO_3]^{+}$				761.2(10)	783.3(5)
$[Ln(NO_3)_2L_3]^{+}$	1127.3(15)	1129.2(10)	1132.4(5)	1140.3(< 5)	
$[Ln(NO_3)_2L_3–EtNO_3]^{+}$				1049.2(15)	1071.3(5)
$[Ln(NO_3)_2L_3–2EtNO_3]^{+}$				958.3(20)	980.3(10)
$[Ln_2(NO_3)_4L_5–3EtNO_3]^{2+}$				858.5(10)	881.0(< 5)
$[Ln_2(NO_3)_4L_5–4EtNO_3]^{2+}$				813.3(15)	834.8(< 5)

[a] m/z values quoted for the most intense peak in the isotope profile and are within ± Da of the theoretical values. The intensity relative to most intense ion is given in parentheses.

as this would also lead to an increase in the coordination number about the metal, thus increasing the steric crowding in 2 : 1 complexes.

The formation of dimeric complexes is consistent with the NMR analysis which indicates major structural changes in the region of europium and is also in accord with the difficulties in isolation of pure compounds for the heavier lanthanides.

2.2.3.3 Electrospray mass spectrometry. Electrospray mass spectra were obtained from methanol solutions of the complexes and the results are presented in Table 4. The low cone voltage spectra are most likely to be representative of the species present in solution and are discussed first. For all the complexes ligand redistribution is apparent with the base peak in the spectra of the complexes La–Nd due to $[LnL_3(NO_3)]^{2+}$. Ions derived from the solid state structure of the complexes such as $[LnL_2(NO_3)_2]^{+}$ are present at moderate intensity. Interestingly, for the complexes of the lighter lanthanides there are no ions which might arise by loss of ethyl nitrate. Raising the cone voltage simplifies the mass spectra with $[LnL_2(NO_3)_2]^{+}$ being the only metal based ion observable. In all the spectra peaks due to $[L + H]^{+}$ and $[L + Na]^{+}$ are observed, and at higher cone voltage decomposition of the ligand by sequential loss of C_2H_4 is observed. The same effect is seen in the spectrum of L itself at higher cone voltages and is not dependent on lanthanide coordination.

As the Yb complex could not be isolated as a pure solid, a solution of $Yb(NO_3)_3$ and L in methanol was used to study the behaviour of the heavier lanthanides. Ytterbium has a characteristic isotope signature and was thus chosen in preference to lutetium. The mass spectra of the samarium and ytterbium complexes are very different from those of the lighter lanthanides. The spectra show peaks due to ions which have lost $EtNO_3$ as the main features in the spectra at +20 V, correspondingly, the base peak is due to $[LnL_3(NO_3)–EtNO_3]^{2+}$. Sequential loss of ethyl nitrate is seen in several series of peaks due to ions such as $[LnL_3(NO_3)_2–nEtNO_3]^{+}$ (n = 1, 2). The assignments are based on the mass to charge ratio and on comparisons of the theoretical and observed isotope profiles which are all in excellent agreement, one example of $[SmL_3(NO_3)_2–2EtNO_3]^{+}$ being shown in Fig. 5. Dimeric ions such as $[Ln_2L_4(NO_3)_5–nEtNO_3]^{+}$ (n = 2–4), $[Ln_2L_3(NO_3)_5–nEtNO_3]^{+}$ (n = 1–4) , $[Ln_2L_5(NO_3)_4–nEtNO_3]^{2+}$ (n = 2–4), $[Ln_2L_4(NO_3)_4–nEtNO_3]^{2+}$ (n = 2, 3) are also observed as peaks of moderate intensity in some cases. The isotope patterns are consistent with Ln_2 based ions and a comparison of the observed and theoretical isotope profiles of $[Sm_2L_4(NO_3)_5–3EtNO_3]^{+}$ is shown in Fig. 6 as a representative example.

Attempts to mimic the loss of ethyl nitrate observed in the mass spectra were made by heating either solutions of lutetium nitrate and ligand in triethyl orthoformate or a neat mixture of the ligand and lutetium nitrate. The infrared spectra of the gas above the reaction mixture held at about 140 °C showed only triethyl orthoformate vapour or no spectrum respectively, with no absorptions due to ethyl nitrate. The stability at these temperatures is consistent with the decomposition temperatures observed in the solid state. Whilst we have unambiguously identified dimeric species in the gas phase decomposition of the complexes of the heavier lanthanides, it is unlikely that the same complexes are formed in solution under ordinary conditions. The dimers formed during the electrospray process

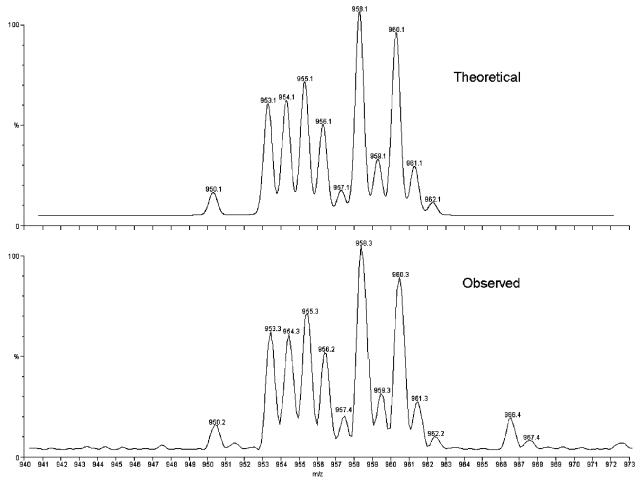

Fig. 5 Theoretical Isotope Profile of $[SmL_3(NO_3)_2–2EtNO_3]^{+}$ and that observed at +20 V cone in the Electrospray Mass Spectrum.

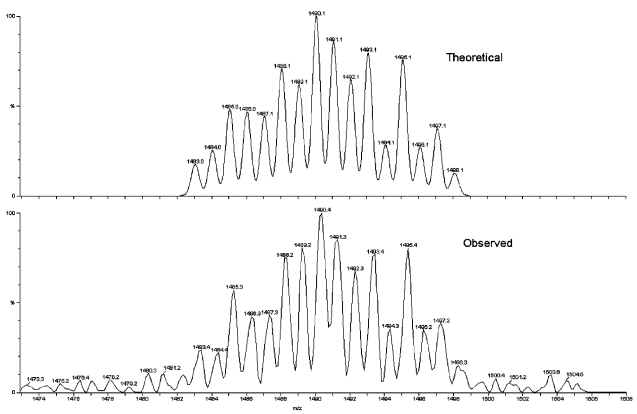

Fig. 6 Theoretical Isotope Profile of $[Sm_2L_4(NO_3)_5–3EtNO_3]^{+}$ and that observed at +20 V cone in the Electrospray Mass Spectrum.

probably contain bridging phosphonate anions rather than neutral bridging bisphosphonate ligands.

3 Conclusion

The solid state structures give an indication of a possible reason for the nascent formation of ethyl nitrate, particularly for the Sm complex, in which intermolecular contacts between nitrate and ethyl groups are strongest. However, we are at present unable to account for why, since the production of ethyl nitrate only occurs on heating the solid complexes to 175 °C, we have difficulties in isolating crystalline materials from solution, wherein the conditions during attempted crystallisations are much less severe, the complexes being subject to temperatures of 100 °C at most. The cut-off point for synthetic availability correlates well with changes in NMR spectra and conductivity; as for the electrospray mass spectra, whilst it may be possible that decomposition by loss of ethyl nitrate may be partly caused by the electrospray process itself, the presence of significant intensity peaks from dimeric species is consistent with an intermolecular reaction producing ethyl nitrate which may operate in addition to any intramolecular one. In this context it is interesting to speculate on whether any parallel exists between the catalytic activity of lanthanide ions in the hydrolysis of DNA[28] and the loss of ethyl nitrate in our systems. Of the two mechanisms thought to be responsible for DNA cleavage P–O bond polarisation by lanthanide coordination seems most likely and the observation of dinuclear species in Ce(IV) induced DNA hydrolysis[29] is mimicked by the observation of bimetallic species in the electrospray mass spectra.

4 Experimental

Infrared spectra were obtained as either KBr discs on an ATI Mattson Genesis FTIR spectrometer or without pretreatment on a Thermo Nicolet AVATAR 370 FTIR. NMR spectra were obtained on a JEOL FX-90Q and conductivity measurements made using a Union Cambridge WPA CM35 conductivity meter.

4.1 Synthesis of $(EtO)_2P(O)CH_2P(O)(OEt)_2$

Stoichiometric amounts of the reagents 12.2 g (70 mmol) CH_2Br_2 and 23.3 g (140 mmol) $(EtO)_3P$ were mixed, heated to boiling, and were allowed to reflux under nitrogen for 1 week. The brown liquid thus produced was fractionated by vacuum distillation. The 130–140 °C fraction (0.5 mm Hg) Lit:[30] 135–137 °C (0.4 mm Hg) was collected, 2.40 g (12%). Infrared spectroscopy: (neat) ν(P=O) 1255 cm^{-1}(s), ν(P–O) 1030 cm^{-1}(s), ^{31}P NMR (neat liquid) δ 19.9 ppm, 19.4 ppm ($CDCl_3$).

4.2 Synthesis of $Ln[(EtO)_2P(O)CH_2P(O)(OEt)_2]_2(NO_3)_3$

Complexes were prepared using trimethyl orthoformate as solvent and *in situ* dehydrating agent. Characterising data are shown in Table 4.

4.2.1 Lanthanum → Samarium. Lanthanide nitrate (~0.5 mmol) was dissolved in 1–2 cm^3 trimethyl orthoformate by gentle warming. The warm solution was added to an appropriate amount (~1.0 mmol) of liquid diphosphonate. After mixing, the solution was allowed to stand for 24 h. The crystallised bis(diphosphonate) complexes were collected by filtration and washed with diethyl ether and dried at the pump. The crystals were found to be suitable for X-ray diffraction studies.

4.2.2 Europium → Gadolinium. No product crystallised spontaneously from trimethyl orthoformate solution. The addition of diethyl ether however precipitated a viscous liquid, which solidified on trituration with diethyl ether. The gadolinium containing material was of a waxy semi-solid consistency.

4.2.3 Terbium → Lutetium. No solid material crystallised from trimethyl orthoformate solution but, again, the addition of diethyl ether precipitated a viscous oil. In each case, the oil showed the characteristic colour of the lanthanide ion. The material could not be solidified on trituration with diethyl ether.

4.2.4 Mass spectrometry. Electrospray mass spectra were obtained by the EPSRC National Mass Spectrometry Service Centre at University of Wales, Swansea as described previously.[31]

4.2.5 X-ray crystallography. Data were collected by the EPSRC National Crystallography Service at the University of Southampton using previously described procedures.[32–34]

For both the La and Sm structures, the positions of the metal atoms were estimated using Patterson methods (SHELXS-97),[35] and all remaining non-H atom positions were obtained through subsequent Fourier syntheses (SHELXL-97).[36] Refinement was by full-matrix least-squares on F^2 data using SHELXL-97[36] from within the WinGX[37] suite of software. An absorption correction[34] was applied to the Sm data.

In both of the structures, all non-H atoms were refined anisotropically. All H atoms were refined at calculated idealised positions (methylene C–H = 0.98 Å, methyl C–H = 0.99 Å). H-atoms in similar functional groups or environments were assigned single, refined isotropic displacement parameters. H-atom displacement parameters were, on reconvergence, 0.037(5) $Å^2$ (La, PCH_2P), 0.070(5) $Å^2$ (La, OCH_2C), 0.096(5) $Å^2$ (La, CH_3), 0.034(14) $Å^2$ (Sm, PCH_2P), 0.052(9) $Å^2$ (Sm, OCH_2C), 0.058(8) $Å^2$ (Sm, CH_3).

In the Sm structure, one of the ethoxy groups was disordered and modelled in two alternative positions with a complementary site occupation factor. The factor was refined to a final value of 0.533. The O–CH_2 bonds of the disordered groups (O(11)–C(8) and O(11)–C(8′)) were restrained to an idealised bond distance of 1.47 Å consistent with the other O–CH_2 bonds in the Sm and La structures.†

Acknowledgements

We are grateful to the EPSRC for use of the X-ray crystallography service at Southampton University and the National Mass Spectrometry Service at Swansea University.

References

1 E. M. Bond, X. Gan, J. R. Fitzpatrick and R. T. Paine, *J. Alloys Compd.*, 1998, **271–273**, 172.
2 X. Gan, E. N. Duesler, R. T. Paine and P. H. Smith, *Inorg. Chim. Acta*, 1996, **247**, 29.
3 R. T. Paine, E. M. Bond, S. Parveen, N. Donhart, E. N. Duesler, K. A. Smith and H. Noth, *Inorg. Chem.*, 2002, **41**, 444.
4 X. M. Gan, E. N. Duesler and R. T. Paine, *Inorg. Chem.*, 2001, **40**, 4420.

† Crystallographic data for the structures reported in this paper have been deposited with the Cambridge Crystallographic Data Centre. Copies of this information can be obtained free of charge from The Director, CCDC, 12 Union Road, Cambridge, CB2 1EZ, UK (*Fax*: +44-1223-336033; *E-mail*: deposit@ccdc.cam.ac.uk; http://www.ccdc.cam.ac.uk). CCDC reference numbers 220337 (Sm) and 220338 (La). See http://www.rsc.org/suppdata/nj/b4/b408536a/ for crystallographic data in .cif or other electronic format.

5 J. H. Matonic, M. P. Nue, A. E. Enriquez, R. T. Paine and B. L. Scott, *J. Chem. Soc., Dalton Trans.*, 2002, 2328.
6 E. M. Bond, E. N. Duesler, R. T. Paine, M. P. Neu, J. H. Matonic and B. L. Scott, *Inorg. Chem.*, 2000, **39**, 4152.
7 Y. M. Kulyako, D. A. Malikov, M. K. Chmutova, M. N. Litvina and B. F. Myasoedov, *J. Alloys Compd.*, 1998, **271–273**, 760.
8 G. Modolo and R. Odoj, *J. Alloys Compd.*, 1998, **271–273**, 248.
9 C. Hill, C. Madic, P. Baron, M. Ozawa and Y. Tanaka, *J. Alloys Compd.*, 1998, **271–273**, 159.
10 T. Yaita and S. Tachimori, *Radiochim. Acta*, 1996, **73**, 27.
11 E. M. Bond, U. Engelhardt, T. P. Deere, R. T. Paine and J. R. Fitzpatrick, *Solvent Extr. Ion Exch.*, 1997, **15**, 381.
12 Y. C. Tan, X. M. Gan, J. L. Stanchfield, E. N. Duesler and R. T. Paine, *Inorg. Chem.*, 2001, **40**, 2910.
13 F. Arnaud-Neu, J. K. Browne, D. Byrne, D. J. Mars, M. A. McKervey, P. O'Hagan, M. J. Schwing-Weill and A. Walker, *Chem. Eur. J.*, 1999, **5**, 175.
14 T. Yaita, H. Narita, S. Suzuki, S. Tachimori, H. Shiwaku and H. Motohashi, *J. Alloys Compd.*, 1998, **271–273**, 184.
15 W. E. Stewart and T. H. Siddall III, *J. Inorg. Nucl. Chem.*, 1968, **30**, 1513.
16 M. Mehring, D. Mansfeld and M. Schürmann, *Z. Anorg. Allg. Chem.*, 2004, **630**, 452.
17 W. E. Stewart and T. H. Siddall III, *J. Inorg. Nucl. Chem.*, 1971, **33**, 2965.
18 A. M. J. Lees, J. M. Charnock, R. A. Kresinski and A. W. G. Platt, *Inorg. Chim. Acta*, 2001, **312**, 170.
19 A. B. P. Lever, E. Mantovani and B. S. Ramaswami, *Can. J. Chem.*, 1971, **49**, 1957.
20 P. Byers, M. G. B. Drew, M. J. Hudson, N. S. Isaacs and C. Madic, *Polyhedron*, 1994, **13**, 349.
21 V. E. Karasev, A. V. Gerasimenko, A. G. Mirochnik, I. N. Botova and N. V. Polyakova, *Russ. J. Coord. Chem.*, 1999, **25**, 885.
22 P. Thuéry, M. Nierlich, M.-C. Charbonnel and J.-P. Dognon, *Acta Crystallogr., Sect. C*, 1999, **55**, 1434.
23 NIST Chemistry WebBook, http://webbook.nist.gov/chemistry/name-ser.html.
24 P. Rubini, C. Ben Nasr, L. Rodhuser and J.-J. Delpuech, *Magn. Reson. Chem.*, 1987, **25**, 609.
25 (*a*) C. F. G. C. Geraldes, S. Zhang and A. D. Sherry, *Inorg. Chim. Acta*, 2004, **357**, 381; (*b*) C. F. G. C. Geraldes, S. Zhang, C. Platas, T. Rodrigues-Blas, A. de Blas and A. D. Sherry, *J. Alloys Compd.*, 2001, **323–324**, 824; (*c*) N. Ouali, J.-P. Rivera, D. Chapman, P. Delagle and C. Piguet, *Inorg. Chem.*, 2004, **43**, 1517.
26 W. J. Geary, *Coord. Chem. Rev.*, 1971, **7**, 81.
27 S. Kannan, N. Rajalakshmi, K. V. Chetty, V. Venugopal and M. G. B. Drew, *Polyhedron*, 2004, **23**, 1527.
28 S. J. Franklin, *Curr. Opin. Chem. Biol.*, 2001, **5**, 201.
29 H. Shigekawa, H. Ikawa, R. Yoshizaki, Y. Iijima, J. Sumoaka and M. Komiyama, *Appl. Phys. Lett.*, 1996, **68**, 1433.
30 G. M. Kosolapoff, *J. Am. Chem. Soc.*, 1953, **75**, 1500.
31 J. Fawcett, A. W. G. Platt and D. R. Russell, *Polyhedron*, 2002, **21**, 287.
32 *Collect – Data collection software*, R. Hooft, B. V. Nonius, 1998.
33 Z. Otwinowski, W. Minor, in *Macromolecular Crystallography, Part A: Methods in Enzymology*, eds. C. W. Carter, Jr. and R. M. Sweet, Academic Press, London, 1997, **Vol. 276**, p. 307.
34 *SORTAV absorption correction software package*: (*a*) R. H. Blessing, *Acta Crystallogr., Sect. A*, 1995, **51**, 33; (*b*) R. H. Blessing, *J. Appl. Crystallogr.*, 1997, **30**, 421.
35 (*a*) G. M. Sheldrick, *SHELXS-97 – A program for automatic solution of crystal structures*, University of Goettingen, Germany, Release 97-2, 1997; (*b*) G. M. Sheldrick, Z. Dauter, K. S. Wilson, H. Hope and L. C. Sieker, *Acta Crystallogr., Sect. D*, 1993, **49**, 18.
36 G. M. Sheldrick, *SHELXL-97 – A program for crystal structure refinement*, University of Goettingen, Germany, Release 97-2, 1997.
37 (*a*) L. J. Farrugia, *WinGX – A Windows Program for Crystal Structure Analysis*, University of Glasgow, 1998; (*b*) L. J. Farrugia, *J. Appl. Crystallogr.*, 1999, **32**, 837.
38 K. Davies, *SNOOPI – Molecular plotting program*, Chemical Crystallography Laboratory, University of Oxford, 1983.